Using Novel Methods to Characterise Slag Films for Continuously Casting Challenging and Innovative Steel Grades

Z.Li[1], T. Zhang[2], S. Qin[3], X. Yang[4], Z. Yan[5], P. Wilson[6] and M. A. Williams[7]

1.Professor, University of Warwick, Coventry CV4 7AL. Email: Z.Li.19@warwick.ac.uk
2.Professor, Shanghai University, Shanghai 200444. Email: Tongsheng_Zhang@shu.edu.cn
3.Research Fellow, University of Warwick, Coventry CV4 7AL. Email: Shiying.qin@warwick.ac.uk
4.Research Fellow, Brunel University London, Middlesex UB8 3PH. Email: Xinliang.yang@brunel.ac.uk
5.Research Fellow, University of Warwick, Coventry CV4 7AL. Email: Zhiming.yan@warwick.ac.uk
6. Research Fellow, University of Warwick, Coventry CV4 7AL. Email: paul.wilson@warwick.ac.uk
7. Professor, University of Warwick, Coventry CV4 7AL. Email: M.A.Williams.1@warwick.ac.uk

Keywords: Steel continuous casting, slag film, characterisation, novel methods, challenging steels

ABSTRACT

Continuous development of complex new steel grades to meet the ever-increasing demand of high performance causes recurrent issues in steel continuous casting such as surface quality defects (e.g. cracks, depressions, deep oscillation marks) and productivity challenges (e.g. faster casting, near-net shape casting). Continuous casting of steel is a highly successful metallurgical process. Much of this success can be attributed to the performance of the casting powder that is added to the top of the mould, creates a liquid slag pool as it is heated, and forms a slag film between the water-cooled copper mould and steel shell during its passage down the mould.

Mould powder selection is a compromise between the conflicting requirements of heat transfer and lubrication. In an EU RFCS (Research Fund for Coal and Steel)-funded project, various techniques are developed to offer the opportunity to adapt the slag film to meet the conflicting needs in different parts of the mould such that mild cooling can be generated in the meniscus, mid-broad face or corner areas whilst maintaining lubrication and offering higher cooling rates in other areas of mould. This has significant potential to address the industrial issues in product quality and productivity of continuous casting.

This paper reports, as part of the EU RFCS project, the determination of crystallinity and porosity in slag films for casting challenging and innovative steel grades using new methods. In comparison with the methods such as XRD analysis and OM/SEM analysis that are currently adopted by the industries, EBSD (electron backscatter diffraction) has been employed to determine the crystallinity of the slag films taken from industry casters. X-ray computed tomography (XCT) plus 3D image reconstruction has been used to determine the slag film %porosity with pore volume, pore size distribution, and pore location, which can be linked with the performance of the slag films during casting different steel grades.

INTRODUCTION

The global crude steel production in 2022 is 1884.2 Mt, 96.8% of which is casted by continuous casting technologies (Worldsteel Association, 2023). The success of the steel continuous casting can be attributed to the performance of the casting powder that is added to the top of the mould, creates a liquid slag pool as it is heated, and forms a slag film between the water-cooled copper mould and steel shell during its passage down the mould. Continuous development of complex new steel grades to meet the ever-increasing demand of high performance causes recurrent issues in steel continuous casting such as surface quality defects (e.g. cracks, depressions, deep oscillation marks) and productivity challenges (e.g. faster casting, near-net shape casting). Therefore, continuous endeavours have been made to develop new mould powders for the continuous casting of such challenging and innovative steel grades.

The slag film between the water-cooled copper mould and steel shell in its initial stage consists of a solid slag layer because of its freezing on the water-cooled copper and a liquid layer next to the high temperature steel shell. This structure fulfils the major functions of the mould powder in the continuous casting – the liquid slag layer provides the right level of lubrication to the steel shell and the solid layer determines the heat flux (i.e. heat transfer from the steel shell to copper mould). Major task for developing new mould powder has always been ensuring its physical and chemical properties (such as viscosity, solidification temperature or break temperature, melting behaviour) to balance the lubrication and horizontal heat transfer and avoid casting problems like longitudinal cracking and sticker breakouts (Sridhar *et al*, 1998). The slag film evolutes during its travelling down the mould. Depending on the steel grades casted and the designed chemistry of the mould powder, the liquid layer solidifies and may crystallise depending on the chemistry and thermal conditions, and the solid layer also crystallises during the thermal processing. The crystals in the slag film scatter infra-red radiation and consequently reduce the heat transfer from the steel shell to copper mould. Therefore, the crystallinity of slag film is a major factor controlling the horizontal heat flux in the mould. (Susa et al, 2009) Pores are also found during the examination of the slag films taken from the industry mould (Li, Millas and Bezerra, 2004) although the formation mechanisms of pores in slag film have not been well understood. The increased porosity also results in the decrease in heat transfer from the steel shell to the mould. (Mills and Dacker, 2017).

In summary crystallinity and porosity are two major characteristics determining horizontal heat transfer from the steel shell to copper mould, which is critically important to cast challenging and new steel grades without defects. This paper investigates the methods for determining the crystallinity and porosity of slag films taken from industrial casting moulds.

CRYSTALLINITY

The initial slag film formed consists of a glassy layer in the water-cooled mould side and a liquid layer in the high-temperature steel shell side. The thin liquid layer solidifies, and the slag film crystallises over time until the crystallinity (f_{crys}) in the slag film reaches a steady state. The crystallinity in the slag film is one of the key parameters controlling the horizontal heat transfer from the steel shell to the mould. As summarised by Mills and Dacker (2017), three major parameters controlling the horizontal heat flux from the shell to mould are (i) the thickness of the slag film, (ii) the fraction of crystalline phase (i.e. crystallinity, f_{cryst}) and the size of the crystallites in the slag film, and (iii) the interfacial resistance between the copper mould and slag film and porosity formed by the shrinkage of slag during crystallisation. One of the major research topics on crystallinity is to manipulate the crystalline phase and consequently control the crystallinity (f_{cryst}) in the slag film. Cuspidine ($3CaO{\cdot}2SiO_2{\cdot}CaF_2$) is the primary crystalline phase in the conventional fluorine-containing casting powders but not in the environmentally friendly fluorine-free mould slag or calcium aluminate mould slags. Increasing the slag basicity (CaO/SiO_2) generally increases its crystallinity. Without being involved in too much detail in the mechanisms of crystallinity in slag film, this chapter focuses on the determination of the crystallinity in slag films taken from industry casting moulds. In this chapter, the authors will first determine the crystallinity of slag films using OM (optical microscopy), SEM (scanning electron microscopy) and XRD (X-ray powder diffraction) techniques, and then explore the use of EBSD (electron backscatter diffraction) in quantitatively analysing the crystallinity (f_{cryst}) of the slag film.

OM (Optical Microscopy) image analysis

The procedure to determine the crystallinity of slag film is to observe the well-prepared slag film sample under optical microscope, select the representative range/area(s) of the slag film for analysis, determine the crystalline and glassy phases, take photos of the selected area(s), and determine the crystallinity based on the estimation of the selected area(s). Figure 1 shows how OM is applied to determine the crystallinity of slag film B. Slag film B has two distinguished layers of glass and crystalline, which enables the researcher to estimate the crystallinity to be around 50%.

The OM analysis can allow large areas of slag film to be analysed. This method is simple to provide comparative information for different slag films. However, this purely depends on the researcher's experience to choose the representative area(s) and distinguish the crystalline and glass phases. If there is no clear boundary between the glass and crystalline phases, or the crystallites scatter in the glassy phase or vice versa, its accuracy will be influenced.

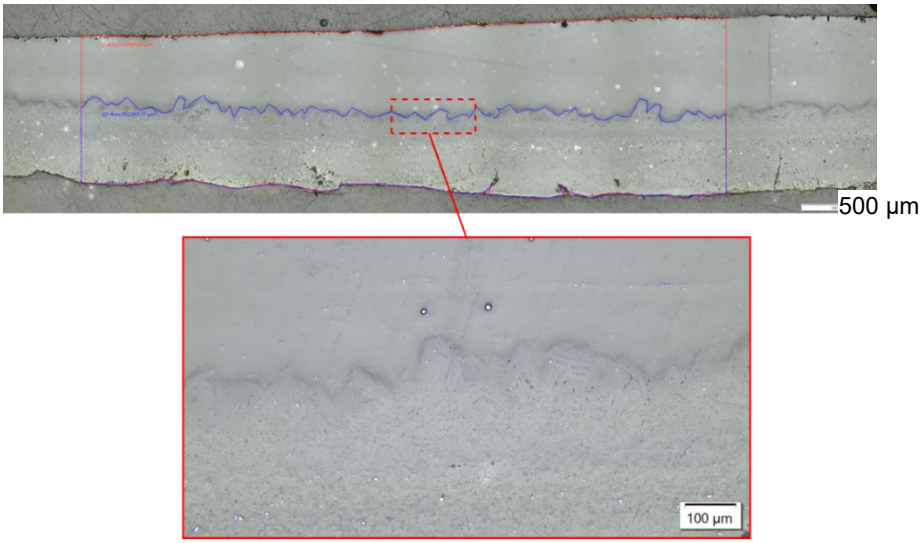

FIG1 – Optical microscope (OM) image of slag film B for crystallinity estimation.

SEM image analysis

The procedure for SEM image analysis is similar to that for OM image analysis. However, SEM can go higher magnification than OM, which enables clear identification of crystalline phases in a focused area. Figure 2 illustrates the slag films A (top), B (middle) and C (bottom) respectively from industry casting moulds. The crystalline phase, glass phase and pores are clearly shown in the figures.

Slag film A has a thin layer in contact with steel shell consisting of crystalline phase (cuspidine), a thick glassy phase next to mould, and pores (Figure 2 top). This thin layer could be the liquid layer in the initial formation of the slag film. Slag film B (Figure 2 middle) composes of two clear, similar thickness layers with the flat, glassy layer in contact with mould. The layer next to the steel shell is mainly crystalline phases (nepheline – $NaAlSiO_4$, cuspidine), pores and iron droplets. Dendrite crystalline is clearly observed to grow at the interface in the direction from the steel shell to the mould. Compared to Figure 1 by OM, SEM image clearly shows the morphology of the slag film. Slag film C (Figure 2 bottom) is mainly crystalline with large pores in the steel shell side.

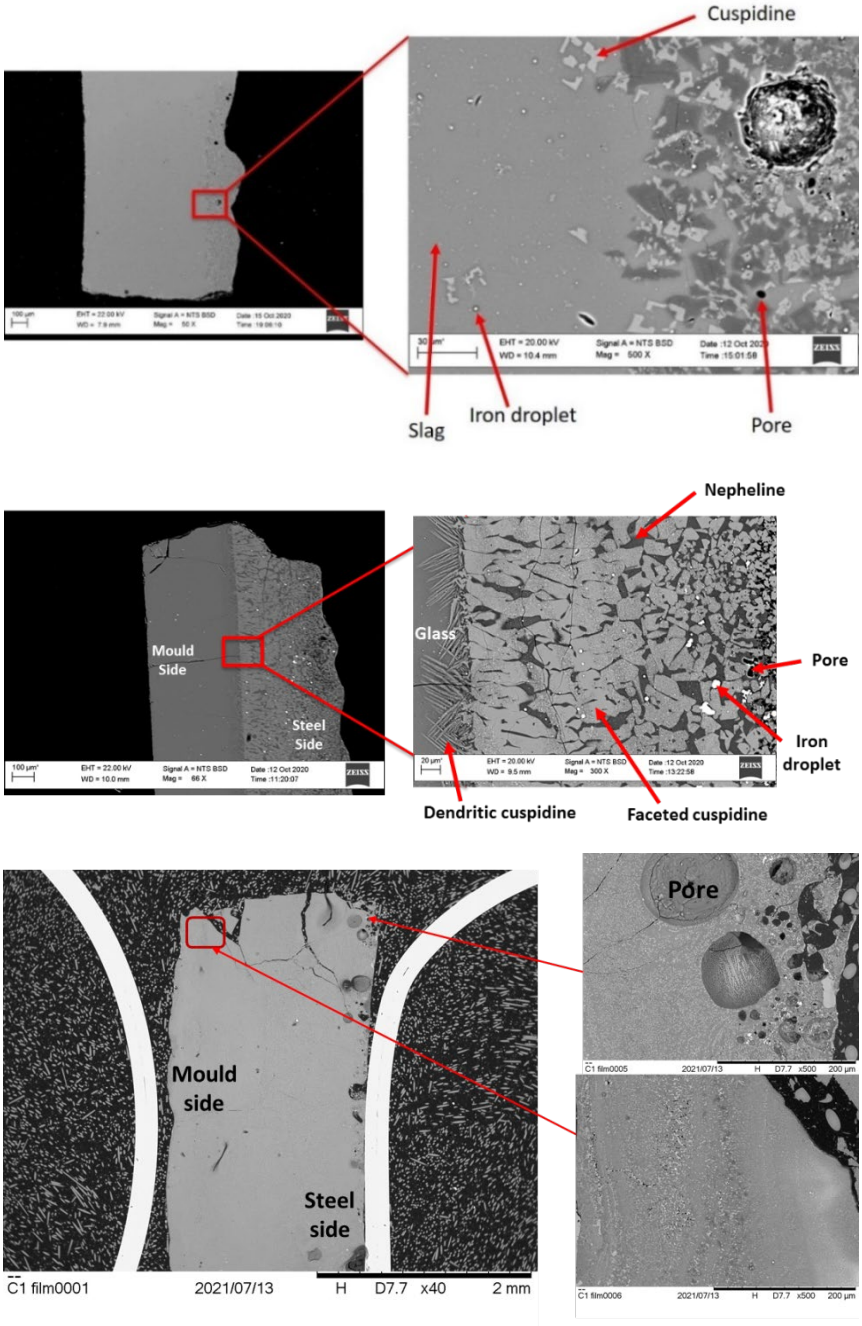

FIG 2 – SEM micrographs of slag films A (top), B (middle) and C (bottom). For each of the slag films, the left is its cross-section image, and the right is the focused area.

SEM image can clearly show the crystalline and glassy phases in the slag films. However, the crystallinity determined is limited to the area(s) tested. Reliable results can only be obtained by examining an area which can represent the slag film. Therefore, macro photos of the whole slag film were taken, for example, as shown in Figure 3(a). Then a thresholded image was obtained with the help of Image J or other similar software, as shown in Figure 3(b). Finally, the crystallinity of the industrial slag film can be calculated according to the color difference, average f_{cryst} is then calculated using Eq. (1).

$$\overline{f}_{cryst} = \frac{\sum f_{cryst} \cdot A_i}{\sum A_i} \quad (1)$$

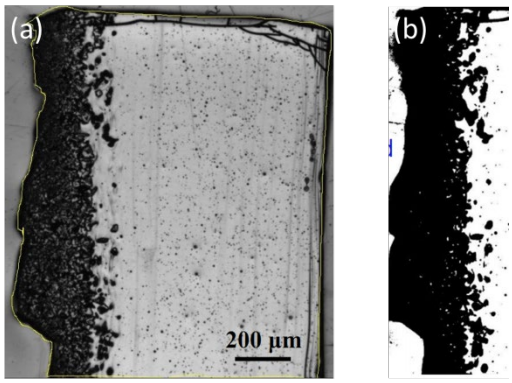

FIG 3 - Analysis process of SEM micrograph of a slag film at higher magnification: (a) SEM micrograph and (b) thresholded image.

Accordingly, the crystallinity determined by SEM image analysis is 21%, 56% and 100% for slag films A, B and C respectively. In summary, OM or SEM can be used to determine the crystallinity of the slag films. The value and accuracy of the crystallinity determined depend on the representative area(s) selected. The difference between crystalline and glass phases may be subject to the researcher's experience. SEM, because of its better identification of crystalline phase, could give better outcomes compared to OM.

XRD analysis

XRD is a proven technique to determine the phases and their quantities in powders. The experimental procedure adopted in this study is to select representative pieces of the slag film and grind them to fine powders for XRD analysis. Panalytical X'Pert Pro MRD™ using a Cu-K_α radiation was employed with an accelerating voltage of 40 kV and a tube current of 40 mA. For XRD scans, the scanning angle was varied from 20° to 80° at a rate of 2°/min.

The type of the crystalline phases in the slag film samples can be obtained by analysing the XRD pattern of the sample, however, this study is more interested in the crystalline phase content (crystallinity f_{cryst}). The diffraction peak of crystal phase presents a high intensity in a narrow degree (i.e. crystalline area), by contrast, the diffraction peak of the glass phase looks like a steamed bread owing to the low intensity and wide degree (i.e. amorphous area). The degree of crystallinity (f_{cryst}) can be determined by the total integrated area of the crystal and glassy phase peaks in the XRD pattern of the sample. The f_{cryst} is then calculated by Eq (2):

$$fcryst = \frac{Crystalline\ Area}{Crystalline\ Area + Amorphous\ Area} \quad (2)$$

Figure 4 is the XRD patterns of three slag film powder samples obtained. For the slag film A, the crystallinity in the mould side and in the steel shell side varies as shown in Figure 4(a). So the selected pieces of a slag film were fully crushed for the XRD test. The crystallinity for the three slag films determined is 22%, 65% and 100% for slag films A, B and C respectively. It is concluded that XRD does provide reasonable, consistent results.

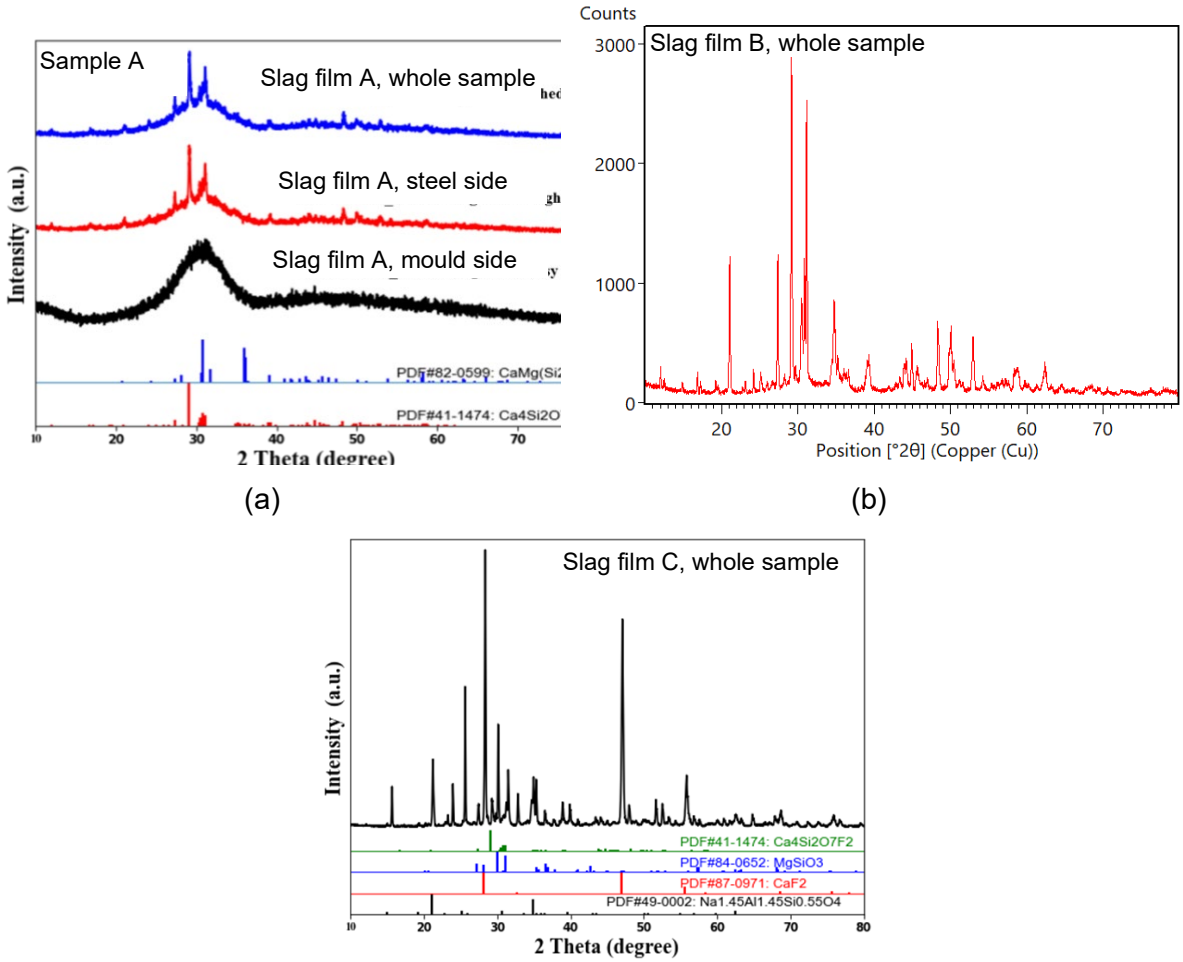

FIG 4 - XRD patterns of three slag film sample powders A, B and C.

EBSD analysis

Electron backscatter diffraction (EBSD), in addition to the conventional techniques of XRD analysis and OM/SEM image analysis, was attempted to obtain the crystallinity of slag film samples. EBSD is a scanning electron microscope-based microstructural-crystallographic characterisation technique commonly used in the study of crystalline or polycrystalline materials, which may be able to provide information about the crystallinity of slag films tested. The industrial slag film C is used as an example for the development. As shown in Figure 5, the presence of many small crystals only 1-2 μm in size (and glass phase if there is) can be detected. The crystalline phases and volumes in the area can be identified by using Kikuchi Patterns in EBSD (Figure 6). The total crystallinity of slag film C is about 71.1%, which is lower than that determined by XRD analysis and SEM image analysis (100%). The main reasons could be, 1) to accurately determine the crystallinity of the slag film sample, pre-setting all the crystalline phases in the tested areas is essential, however, some minor phases in the tested areas might not be determined before EBSD analysis, and 2) the areas tested may not be sufficient in size. All these factors can be further improved.

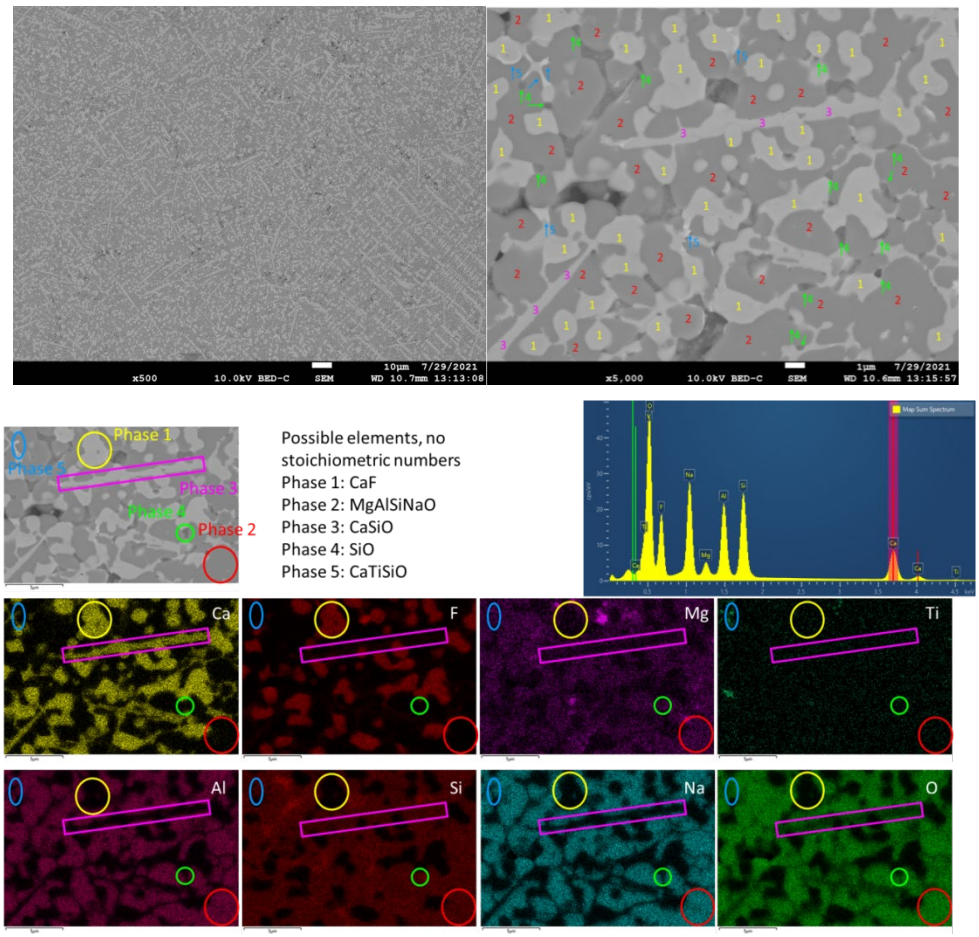

FIG 5 – SEM micrographs and the types of small size crystalline phases in slag film C. (Phase 1: CaF_2, Phase 2: MgAlSiNaO. Phase 3: CaSiO Phase 4: SiO Phase 5: CaTiSiO)

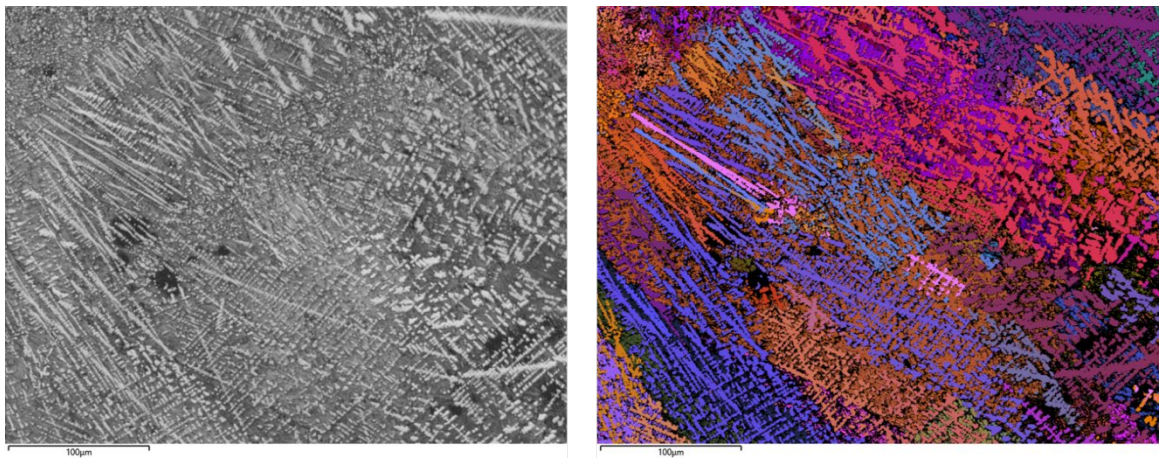

FIG 6 – Identification of crystalline phases using Kikuchi patterns in EBSD. Examination area: 0.4 mm x 0.3 mm, Step size: 0.5 mm, 503930 points measured in total. Acquisition time: 7 min.

By comparing the crystallinity results from three methods of SEM image analysis, XRD analysis, and EBSD analysis, it can be concluded that the values obtained by XRD analysis and SEM image analysis are in reasonably good agreement. The result from EBSD analysis is lower, which could be further improved by presetting all the crystalline phases in the tested area before EBSD scanning and increasing the size of areas. The advantage of SEM image analysis is its clear indication of crystallinity variation with position (tested area), however, due to the limitation of the field of vision, the results of different planes may have a large deviation. To obtain a reliable result, selecting representative area(s) is the key. XRD analysis, partially because of its easiness in selecting representative samples, may be more suitable for the overall crystallinity analysis of slag film samples.

POROSITY

The porosity in the slag film can come from various sources although it is not well understood. Crystal is denser than glass, so crystallisation results in shrinkage and consequently creates micro-pores in the slag film. However, crystallisation is not the only cause of porosity. Casting powder with a high moisture content (or water leaks) can lead to hydrogen pores in the slag film. Blowholes containing $CO_{(g)}$ can be formed from reaction of C and FeO in the slag. (Mills and Dacker, 2017) Also the potential reactions within the mould flux at high temperature such as evaporation of CaF_2 and formation of SiF_4 in fluorine-containing mould powder can also form pores. Different morphologies of pores have been observed in industrial slag films, which could be attributed to different formation mechanisms.

Mould flux is distributed between the mould and steel shell, which controls heat transfer and lubrication during continuous casting. The porosity in the slag films has a great influence on the heat transfer from the steel shell to the mould, and consequently affects the casting process and quality of the casting products. The increased porosity could lead to a decrease in heat flux from the shell to mould and to sticker breakouts. Because of the importance of porosity in controlling heat flux, Hunt and Stewart (2016) reported that the use of intumescent coatings on the copper mould could reduce heat transfer by up to 27% in a laboratory cold finger simulation experiment.

Although the importance of porosity in slag film in heat flux is well known, their formation mechanisms are not very clear, and the method to determine the porosity is not well established. In this chapter, the authors investigate the methods to determinate the porosity of industrial slag films using techniques from the OM/SEM image analysis to the innovative x-ray computed tomography (XCT) technique for 3-dimensional porosity determination. The number, size and distribution of the pores quantified in the three industrial slag films (A, B and C) are summarized in this section.

SEM image analysis

As shown in Figure 7, by applying appropriate threshold, SEM image (Fig. 7(a)) can be processed to 2D image (Fig. 7(b)) showing the porosity. The porosity in the thresholded image can be obtained by using commercial software such as Image J.

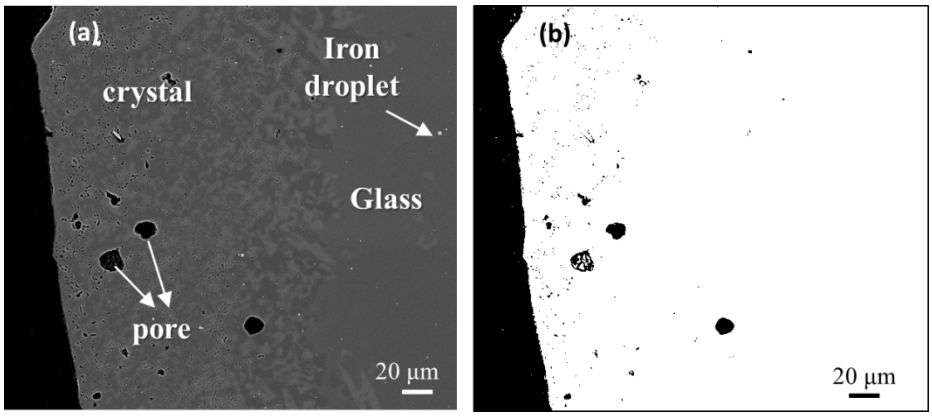

FIG 7 – SEM micrograph of slag film A at higher magnification: (a) SEM micrograph; (b) Thresholded image.

As shown in Figure 8, small pores observed in SEM images of slag film C at high magnifications could be formed during crystallisation compared to the large blowholes observed in Figure 7 for slag film A. Using the SEM method, potentially pores in a wide range of size can be measured in a slag film, which may not be possible in the OM image analysis (which is not included in this paper).

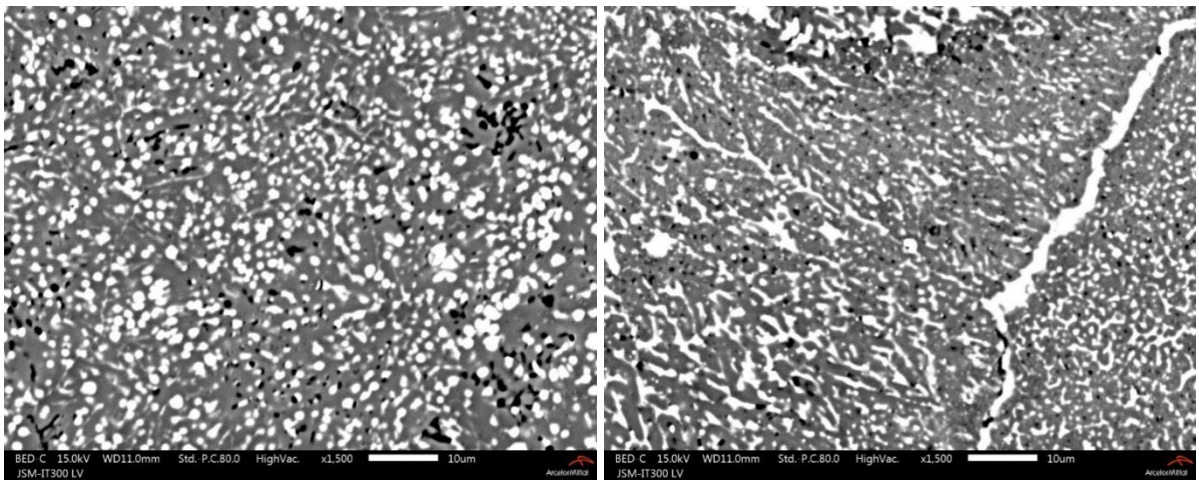

FIG 8 – SEM images at high magnification showing the pores (black spots) in the slag film C probably formed during crystallisation.

The characteristics of porosity in the three slag films A, B and C analysed by the above method are summarised in Figure 9. It should be pointed out that the analyses include all the pores in large areas from 16.18 mm^2 (slag film A) to 22.70 mm^2 (slag film C). The porosity obtained is 3.31% (slag film A), 1.83% (Slag film B) and 4.24% (slag film C), respectively.

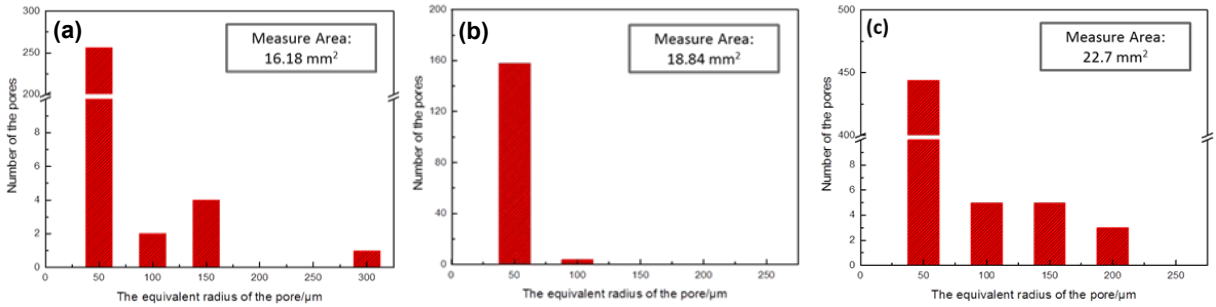

FIG 9 - Size distribution of all internal porosities in industrial slag films (a) B, (b) A, and (c) C. The equivalent radius of the pore is calculated by assuming the pore is circle. Radius 50 μm refers to the pores with radius between 0 and 50 μm, and radius 100 μm refers to the pores with radius between 50 and 100 μm, and so on. Measured area refers to the size of area measured for the %porosity.

Big difference in the %porosity even for the same slag film determined by different researchers was observed. The possible reasons are 1) the difficulty to balance the measurement area and accuracy due to the characteristics of the thresholded image detection; and 2) the selected areas – the size of the area and the representative of the area.

XCT analysis

X-ray Computed Tomography (XCT) is a non-destructive technique for visualizing interior features within solid objects, and for obtaining digital information on their 3-D geometries and properties. An XCT image is typically called a slice, as it corresponds to what the object being scanned would look like if it were sliced along a plane. A complete volumetric representation of an object can then be obtained by acquiring a continuous set of CT slices. In the current study, XCT is used as a novel characterisation technique to visualise the slag films in 3D and identify the pores along with their size distribution. The XCT has the capability of identifying pores of very small dimensions with spatial resolutions of ~1/1000 times the thickness of the slag films. The samples used in the XCT tests are in ~20 mm square or round shape (which could be considered representative) cut from the industrial slag film samples. In this study, a lab-based CT scanner (Zeiss 620 Versa CT system) is used for scanning the industrial slag films prepared. The exposure voltage is 80 kV, exposure power 10 W, and exposure time 10 s. The Voxel size is 9.0895 μm. The number of projections is 3201. Imaging processing including filtering, segmentation and quantification were carried out using the Avizo Software (Thermo Fisher Scientific). As an example, Figure 10 shows the morphologies of the slag

film C and porosity in 3D images. From this 3D images, the porosity (%) and pore size distribution can be calculated, and the pore distribution across the sample can be observed.

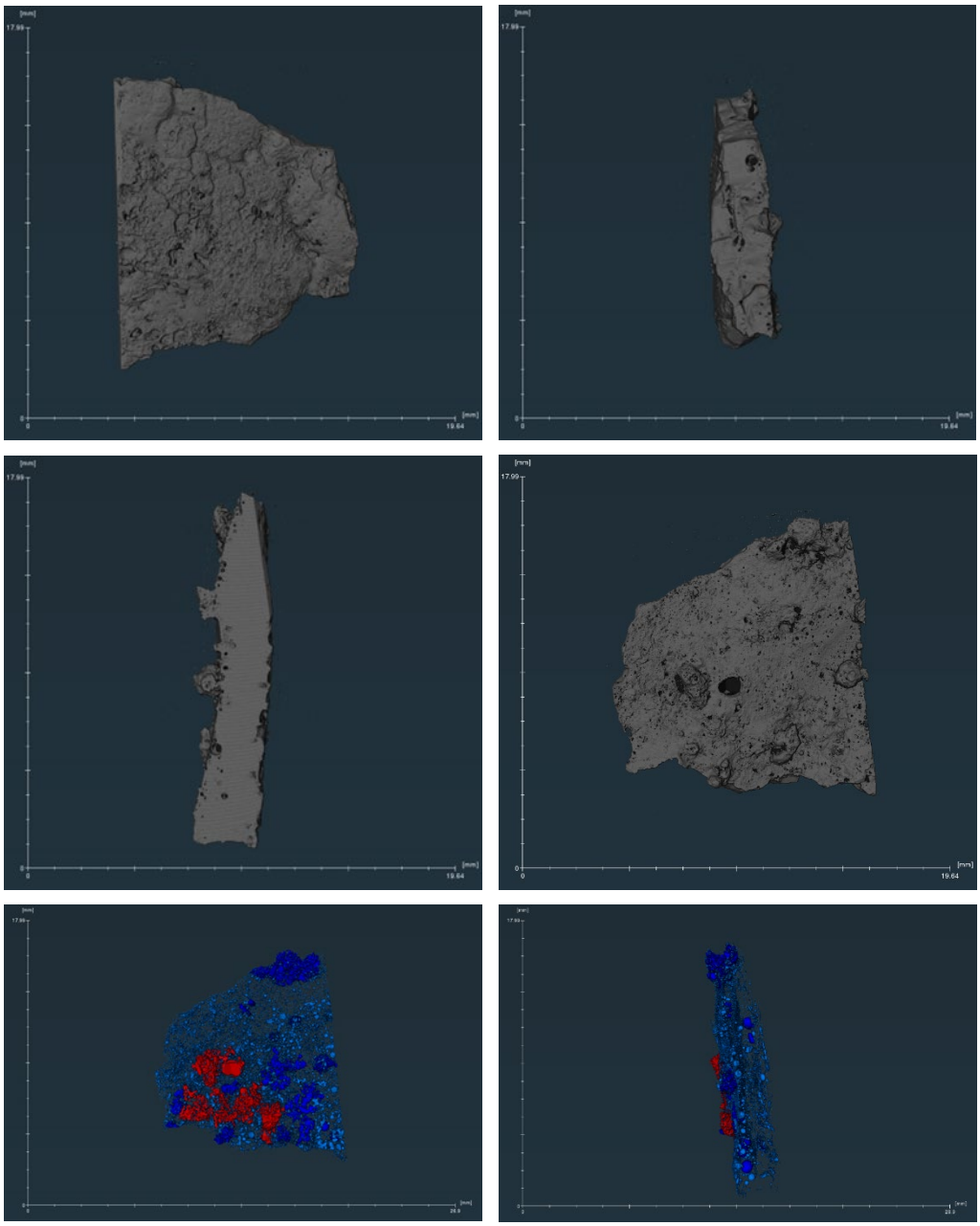

FIG 10 – XCT results for slag film C: morphology (top and middle), and pore distribution in 3D images (bottom).

The number of pores measured by XCT is large (3880 for slag film A sample, 539 for slag film B sample, and 9344 for slag film C sample), which makes the data more truly reflect the characteristics of slag films. The measurement accuracy of XCT is 5 μm in this study, so the statistics range from 5 μm to 500 μm with intervals of 50 μm.

It was found that the sizes of all internal pores in slag film B are smaller than 100 μm, and the proportion (number density percentage) of porosities with radius smaller than 50 μm is above 99%. For slag film A, although the ratio (i.e. number density percentage) of the porosities smaller than 50 μm reached 98%, their volume percentage is less than 7.5%. The larger pores between 50 and 400 μm account for 92.5% of the total volume of pores. Similar phenomena are observed for slag film C. In slag film C, the proportion (number density percentage) of pores with radius below 50 μm almost reaches 60%, but its volume percent is only about 3%. The proportion of pores with a radius of 50-100 μm accounts for about 35%, and the volume percent accounts for more than 20%. In other words, the larger pores (>50 μm) contributes more to its volume ratio. The proportion of varying pores detected by XCT agrees with that by SEM (Figure 9), at least in trend.

Overall, the pores in industrial slag film B are the smallest in all cases, both in average radius (20 μm) and volume ratio (0.05%). The proportion of pores in industrial slag film A is obviously larger than that in slag film B with the average radius 35 μm and porosity 0.7%. The effect of pores in slag film C is more significant. The proportion of pore volume in slag film C is 3% (average pore radius 85 μm), being one order of magnitude larger than that of slag films A and B.

CONCLUSIONS

The authors have explored various methods to determine the crystallinity (f_{cryst}) and porosity (%) of the industrial slag film samples, and the following conclusions can be obtained:

- OM/SEM can be used to determine the crystallinity of the slag film samples and the results does give similar trend to the XRD method. The value and accuracy depend on the representative area(s) selected.
- XRD does provide reasonably consistent results of the crystallinity of slag films.
- EBSD can be a useful tool to determine the crystallinity of the slag film samples, but further development is required for the application.
- The porosity can be measured by using SEM + image analysis, however, variation for the same sample occurs with different researchers. The possible reasons are 1) the difficulty to balance the measurement area and accuracy due to the characteristics of the thresholded image detection; and 2) the selected area(s) to test.
- XCT has the advantages of determining %porosity, pore volume, pore size distribution, and pore location (steel side or mould side). This could be a useful technique for porosity determination in slag film samples.

ACKNOWLEDGEMENTS

The authors would like to acknowledge the financial assistance received from the Research Fund for Coal and Steel (RFCS) under the Grant Number RFCS-2018-847269. The authors also would like to thank the partners in the project for providing industry slag films and discussions – Sidenor Aceros Especiales S. L., ArcelorMittal Maizières Research, SSAB, Sandvik Materials Technology, Proximion, the Materials Processing Institute, Swerim, and the Open University.

REFERENCES

Hunt, A, and Stewart, B, 2016. Techniques for controlling heat transfer in the mould-strand gap in order to use fluoride free mould powder for continuous casting of peritectic steel grades, in *Proceedings of the 10th Internal conference on molten slags, fluxes and salts (MOLTEN16)* (ed: R. G. Reddy, P. Chaubal, P. C. Pistorius, and U. Pal), (The Minerals, Metals & Materials Society.

Li, Z, Mills, K, C, and Bezerra, M, C, 2004. Characteristics of mould flux films for casting MC and LC steels, in *Anais do XXXVI Seminário de Fusão, Refino e Solidificação dos Metais,* pp. 13-24.

Mills, K, C, and Dacker, C. -A, 2017. The casting powders book. (Springer: Switzerland AG). ISBN 978-3-319-53614-9.

Sridhar, S, Mills, K, C, Ludlow, V, and Mallaband, S, T, 1998. A comparison of the mould powders used to cast slabs, billets and blooms, In *Proceeding of the 3rd European Conference on Continuous Casting*, pp 807-816.

Susa, M, Kushimoto, A, Toyota, H, Hayashi, M, Endo, R, and Kobayashi, Y, 2009. Effect of both crystallisation and iron oxides on the radiative heat transfer in mould fluxes, ISIJ International, 49(11), pp. 1722-1729.

Worldsteel Association: World Steel in Figures 2023. https://unesid.org/descargas_files/World-Steel-in-Figures-2023.pdf